Proceedings of the 2014 Joint Rail Conference
JRC2014
April 2-4, 2014, Colorado Springs, CO, USA

JRC2014-3775

ANALYSIS OF THE RELATIONSHIP BETWEEN RAIL SEAT LOAD DISTRIBUTION AND RAIL SEAT DETERIORATION IN CONCRETE CROSSTIES

Matthew Greve
University of Illinois at Urbana-Champaign
Department of Civil and Environmental Engineering
205 N Mathews Ave
Urbana, IL 61801
greve1@illinois.edu

Marcus S. Dersch
University of Illinois at Urbana-Champaign
Department of Civil and Environmental Engineering
205 N Mathews Ave
Urbana, IL 61801
mdersch2@illinois.edu

J. Riley Edwards
University of Illinois at Urbana-Champaign
Department of Civil and Environmental Engineering
205 N Mathews Ave
Urbana, IL 61801
jedward2@illinois.edu

Christopher P. L. Barkan, PhD
University of Illinois at Urbana-Champaign
Department of Civil and Environmental Engineering
205 N Mathews Ave
Urbana, IL 61801
cbarkan@illinois.edu

Jose Mediavilla
Amsted RPS
8400 W 110th St, Suite 300
Overland Park, KS
jmediavilla@amstedrps.com

Brent M. Wilson
Amsted Rail
1700 Walnut St
Granite City, IL 62040
bwilson@amstedrail.com

ABSTRACT

One of the most common failure modes of concrete crossties in North America is the degradation of the concrete surface at the crosstie rail seat, also known as rail seat deterioration (RSD). Loss of material beneath the rail can lead to wide gauge, rail cant deficiency, and an increased risk of rail rollover. Previous research conducted at the University of Illinois at Urbana-Champaign (UIUC) has identified five primary failure mechanisms: abrasion, crushing, freeze-thaw damage, hydro-abrasive erosion, and hydraulic pressure cracking. The magnitude and distribution of load applied to the rail seat affects four of these five mechanisms; therefore, it is important to understand the characteristics of the rail seat load distribution to effectively address RSD.

As part of a larger study funded by the Federal Railroad Administration (FRA) aimed at improving concrete crossties and fastening systems, researchers at UIUC are attempting to characterize the loading environment at the rail seat using matrix-based tactile surface sensors (MBTSS). This instrumentation technology has been implemented in both laboratory and field experimentation, and has provided valuable insight into the distribution of a single load over consecutive crossties. A review of past research into RSD characteristics and failure mechanisms has been conducted to integrate data from field experimentation with existing knowledge, to further explore the role of the rail seat load distribution on RSD. The knowledge gained from this experimentation will be integrated with associated research conducted at UIUC to form the framework for a mechanistic design approach for concrete crossties and fastening systems.

INTRODUCTION

As the demands placed on North American railroad infrastructure continue to increase, and environmental restrictions on timber tie preservation and disposal become more stringent, the use of concrete crossties has become increasingly more prevalent. Concrete crossties are typically used in areas of high curvature, steep gradients, and high annual gross tonnage to reduce maintenance cycles [1]. However, concrete crossties and their premium fastening systems have experienced various material and design failures leading to restricted adoption within the industry. Among the failure methods associated with concrete crossties and fastening systems, rail seat deterioration (RSD) presents one of the greatest concerns. According to a survey of North American Class I freight railroads conducted by researchers at the University of Illinois at Urbana-Champaign (UIUC), RSD was

ranked as the most critical problem with concrete crossties and fastening systems [2]. RSD is defined as the loss of material from the concrete crosstie beneath the rail, and is exacerbated by the demanding loading environments in which concrete crossties are typically deployed [3,4]. RSD typically manifests as a triangular loss of material, with depth of wear increasing towards the field side of the rail seat (Figure 1). This loss of material can result in loss of rail cant, wide gauge, and increased risk of rail rollover, creating an unsafe operation condition [1].

FIGURE 1. EXAMPLE OF RAIL SEAT DETERIORATION

Because RSD is viewed as the most critical challenge with concrete crossties and fastening systems, multiple groups have undertaken research to better understand the causes and mechanisms of RSD.

RSD FAILURE MECHANISMS

Extensive research has been conducted in the past to identify potential failure mechanisms of rail seat deterioration and determine the feasibility of these mechanisms. Initial research at UIUC identified five potentially feasible RSD failure mechanisms: abrasion, crushing, freeze-thaw cracking, hydraulic pressure cracking, and hydro-abrasive erosion. Further research at UIUC has been conducted to examine the feasibility of hydraulic pressure cracking and hydro-abrasive erosion, and to better understand the complex mechanisms of abrasion and freeze-thaw cracking [1,5]. Recently, researchers at the UIUC have undertaken a project in which some of the findings will lead to improvements within the American Railway Engineering and Maintenance of Way Association (AREMA) recommended practices for the design of concrete crossties and fastening systems.

In addition to research at UIUC, the John A. Volpe National Transportation Systems Center (hereafter referred to as "Volpe") modeled RSD to evaluate its consequences on track geometry. The work concluded that under high lateral loads, the rail could rotate, creating a pressure concentration at the field side which could exceed the crushing strength of the concrete [4].

Of the five potential failure mechanisms determined, four (abrasion, crushing, hydro-abrasive erosion, and hydraulic pressure cracking) are affected by the load distribution at the concrete crosstie rail seat. More specifically, these failure mechanisms may be exacerbated by high rail seat stresses resulting from load concentration [1]. Therefore, it is important to understand the rail seat load distribution in order to address RSD as a failure mechanism.

INSTRUMENTATION TECHNOLOGY

To better understand the loading environment at the crosstie rail seat, researchers at UIUC have utilized matrix-based tactile surface sensors (MBTSS). The MBTSS system used by the UIUC is manufactured by Tekscan® Inc. and consists of rows and columns of conductive ink which, when pressed together by a load applied normal to the contact plane, output a change in resistivity at each intersection of a row and a column. This output, termed a "raw sum", can be interpreted as the pressure exerted on the sensor at a given intersection when given the total load applied to the sensor. MBTSS simultaneously outputs the area over which this load is applied. This output, the "contact area" of the load, is calculated from the number of sensing locations which indicate an applied load. Data is collected from the entire sensing area at a maximum rate of 100 Hz.

Previous experimentation at the University of Kentucky (UK) and UIUC have shown that MBTSS are susceptible to shear and puncture damage. To protect the sensors, layers of biaxially-oriented polyethylene terephthalate (BoPET) and polytetrafluoroethylene (PTFE) are secured to both sides of a sensor that has been trimmed to fit the rail seat. The assembly is then installed between the rail pad assembly and the concrete crosstie rail seat (Figure 2) [6].

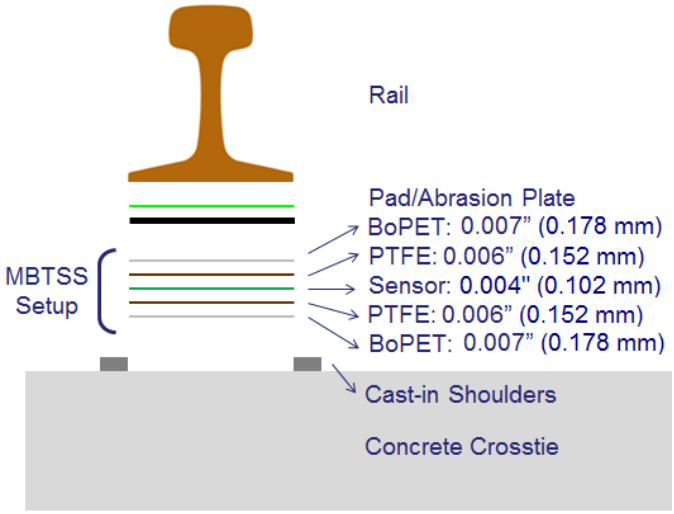

FIGURE 2. MBTSS LAYERS AND THICKNESSES [6]

FIELD EXPERIMENTATION

Field experimentation was performed at the Transportation Technology Center (TTC) in Pueblo, Colorado, USA; a research and testing facility that consists of 48 miles (77.2 km) of railroad track with variable geometries and operating conditions. A section of 15 new concrete crossties was installed on the 13.5 mile (21.7 km) Railroad Test Track (RTT) in a section of tangent track. Eight rail seats, on five crossties, at this site were instrumented with MBTSS (Figure 3). Five consecutive rail seats (near rail seats 1N through 5N) were chosen in an attempt to fully capture the vertical load distribution, and to investigate the effect and variability of support conditions in a group of crossties. Additionally, three consecutive rail seats on the opposite rail (far rail seats 2F through 4F) were selected to provide further information on load transfer, and to examine the variability of support conditions across a single crosstie.

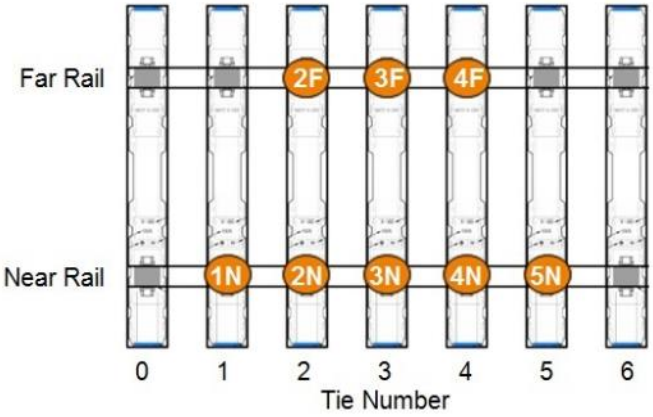

FIGURE 3. PLAN VIEW OF MBTSS FIELD INSTALLATION AT TTC

The loads were applied to the rail using the Track Loading Vehicle (TLV). The TLV is owned by the Association of American Railroads (AAR) and operated by the Transportation Technology Center, Inc. (TTCI). The TLV can be used to study a variety of applications including wheel climb derailments, vertical modulus, lateral track strength, gage widening, and wheel/rail force relationships [7]. An instrumented bogie is attached to vertically- and laterally-oriented actuators, which are attached to the frame of a modified rail car. The TLV's ability to apply controlled vertical and lateral loads to the rail using realistic loading conditions and application made it an ideal tool for the purposes of this experimentation.

The testing procedure consisted of applying loads to both rails with the TLV loading axle centered above each instrumented crosstie. Vertical loads were applied to each rail at increasing magnitudes from 0 to 40,000 lb (178 kN) at 5,000 lb (22.2 kN) increments. At 20,000 lb (88.9 kN) of vertical load, lateral loads were applied at increasing magnitudes from 0 to 12,000 lb (53.4 kN) at 2,000 lb (8.89 kN) increments, resulting in L/V force ratios ranging from 0 to 0.6. The lateral loads were then reduced to zero and a 40,000 lb (178 kN) vertical load was applied to each rail, at which time lateral loads were applied at increasing magnitudes from 0 to 22,000 lb (92.5 kN) at 4,000 lb (17.8 kN) increments, with a final increment of 2,000 lb (8.89 kN), resulting in L/V force ratios ranging from 0 to 0.55. This loading regime was then repeated over each instrumented crosstie.

MODELING RAIL SEAT LOAD ECCENTRICITY

To better understand the cause of RSD's signature triangular wear pattern, Volpe modeled the effect of lateral load on the rail seat load distribution [4]. The rail and rail seat are assumed to be infinitely stiff bodies, and concepts from the design of building footings are used to describe the change in load distribution as lateral load increases. Volpe considered the eccentricity of the overturning moment about the center of the rail base, and determined that if the eccentricity is within the middle third of the base (i.e. the absolute value of the eccentricity is less than or equal to one-sixth the width of the rail base), the load distribution is trapezoidal, as described by Equations (1) and (2). If the eccentricity is beyond the middle third of the rail base, the distribution is triangular, as described by Equation (3) [4].

$$p_g = \frac{P}{b}\left(1 - \frac{6e}{b}\right) \quad (1)$$

$$p_f = \frac{P}{b}\left(1 + \frac{6e}{b}\right) \quad (2)$$

$$p_f = \frac{2P}{3\left(\frac{b}{2} - e\right)} \quad (3)$$

Where p_g = Pressure on gauge side of rail base
p_f = Pressure on field side of rail base
P = Centerline vertical load
b = Rail base width
e = Eccentricity is the applied moment divided by the vertical load (M/P) [4]

We see that the critical eccentricity, at which the gauge side of the rail seat becomes unloaded, is one-sixth the width of the rail base, as described above. Furthermore, we can redefine the expression for eccentricity in terms of the applied lateral and vertical loads and the lever arms with which they act, respective to the centerline of the rail base (Equation 4). Although the authors did not specify an equation to convert lateral load into an overturning moment, they did state that they assumed that the fasteners provided no contribution to the moment [4]. Thus, we can assume that the only contributions to the moment are the lateral load and vertical load eccentricities. We rearrange Equation (4) to obtain an expression for the critical L/V force ratio (Equation 5). We can examine the effect of a load directly above the rail seat of interest, and assume that both the lateral and vertical loads are applied at the gauge face of the rail.

$$e_{crit} = \frac{b}{6} = \frac{M}{P} = \frac{L * h_g - V * \frac{w_h}{2}}{V} \quad (4)$$

$$\frac{L}{V_{crit}} = \frac{\frac{b}{6} + \frac{w_h}{2}}{h_g} \quad (5)$$

Where e_{crit} = Critical eccentricity resulting in triangular load distribution
b = Rail base width
M = Applied moment relative to rail base center
P = Centerline vertical load
L = Applied Lateral load
V = Applied Vertical load
h_g = Height from rail base to gauge face
w_h = Width of rail head

We can apply the dimensions of a 136RE rail section, the size used in field experimentation at TTC, to obtain a critical L/V force ratio of 0.37. At this value, the gauge side of the rail seat will become unloaded, and the load distribution will develop a significant concentration on the field side of the rail seat.

We can now compare this value to results from field experimentation with MBTSS. We see that all eight rail seats experience a loss of contact area at a "threshold" L/V ratio. When a 40,000 lb (178 kN) vertical load is applied, we see that this threshold L/V occurs between 0.3 and 0.4, which agrees with the calculated critical L/V from the Volpe model (Figure 4). However, when the vertical load is reduced to 20,000 lb (88.9 kN), we see that this threshold L/V now occurs between 0.2 and 0.3: our predicted critical L/V now overestimates this threshold (Figure 5).

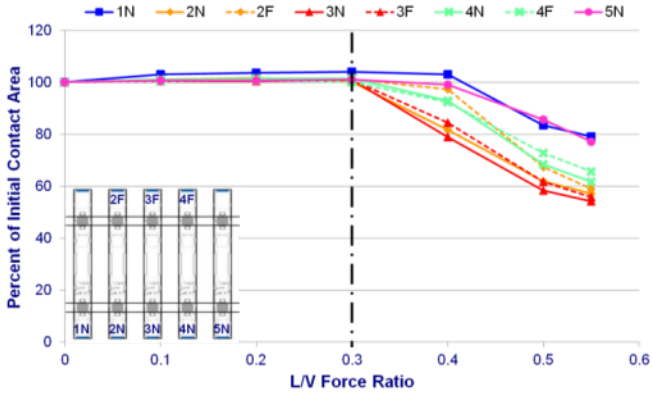

FIGURE 4. LOSS OF CONTACT AREA UNDER 40,000 LB (178 KN) VERTICAL LOAD

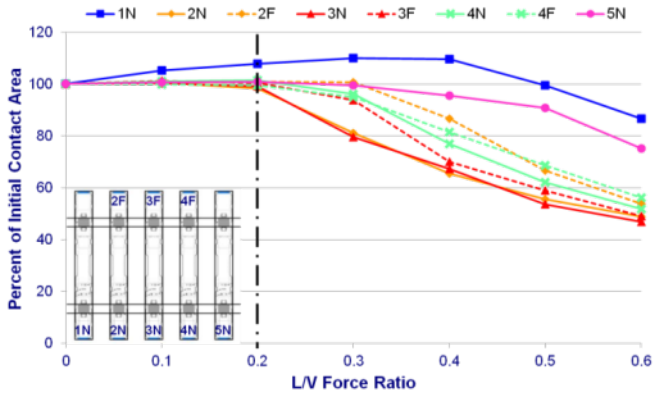

FIGURE 5. LOSS OF CONTACT AREA UNDER 20,000 LB (88.9 KN) VERTICAL LOAD

A possible explanation for this behavior could be derived from the reaction against the lateral load. A higher vertical force would increase the capacity of frictional forces at the rail base-rail pad interface which counters the lateral wheel load. At the critical L/V force ratio, the lateral load may overcome this frictional force and slip to bear against the insulator post and cast-in shoulder. Once this slip occurs, this new bearing point may become a pivot about which the rail can rotate. A lower vertical wheel load would reduce the capacity of the rail pad frictional force, resulting in slip at a lower lateral load.

A second contributing factor could be the location of the contact patch. Below the threshold L/V, the contact patch is located on the head of the rail rather than the gauge face, and only shifts once the lateral load overcomes frictional forces at the wheel/rail interface. Under a 20,000 lb (88.9 kN) vertical load, these frictional forces would be reduced, meaning that less lateral load is required to cause the wheel to slip laterally, reducing the lever arm with which the vertical load is acting to resist the overturning moment. More detailed analysis of the resisting moments applied by the vertical wheel load and fastening system toe loads could further refine this model.

CONTACT PRESSURE AND ABRASION

Researchers at UIUC conducted several representative tests to examine the effect of abrasion on interactions at the rail pad-rail seat interface. These tests involved the construction of a bi-axial loading frame which could apply vertical and lateral loads to specimens representing rail pads of varying material and rail seats. To establish a loading regime, they calculated the average pressure on a rail seat, assuming uniform load distribution over the entire rail seat. This value was estimated to be between 400 psi and 1,800 psi (2.76 MPa and 12.41 MPa, respectively), depending on the applied vertical load. Their findings indicated that in all loading cases, a specimen of nylon 6-6 (a typical rail pad material) will produce abrasion given repeated, small-displacement slip at the rail pad-rail seat interface [5].

To compare this assumption to data from field experimentation, we will examine the change in rail seat pressure at Rail Seat 3N. We will assume Rail Seat 3N supports half of the vertical wheel load applied directly above, and that the other half is distributed within two crossties to either side of the point of loading. This approximation is derived from both experimental field data and literature reviews on rail seat load magnitudes [8]. Therefore, for a 40,000 lb (178 kN) vertical wheel load, we can approximate the total rail seat load as 20,000 lb (88.9 kN), which will remain constant as the L/V force ratio increases.

We can consider three different quantifications of pressure: uniform, average, and maximum. Uniform pressure is calculated by the same method as was used to determine input loads for the previously mentioned abrasion tests: the rail seat load is distributed uniformly over the entire bearing area of the rail seat. Average pressure is calculated by distributing the rail seat load over the observed contact area, the portion of the rail seat which is actually loaded during a given test. Maximum pressure is calculated by determining the conversion factor between the total raw sum recorded by MBTSS and the input load, and then applying this conversion factor to the sensing location with the highest raw sum.

We can now plot the uniform, average, and maximum pressure at a constant vertical load, and examine the effect of increasing the L/V force ratio (Figure 6). By definition, the uniform pressure is unaffected by the change in L/V and remains constant at 556 psi (3.83 MPa), because it assumes that the contact area does not change. Below the previously observed threshold L/V (between 0.3 and 0.4), average pressure plots very close to the uniform pressure, indicating that the entire rail seat is loaded. Beyond the threshold L/V, average pressure increases 71% to 950 psi (6.55 MPa), or 71% greater than the uniform pressure. The maximum pressure is considerably higher than both the uniform and the average pressures, starting at 1,122 psi (7.74 MPa), or 102% greater than the uniform pressure. It increases quadratically to 2,216 psi (15.28 MPa) at 0.5 L/V, a 98% increase from the 0 L/V case, or 299% higher than the uniform pressure. Though not illustrated in Figure 6, the location of the maximum pressure trends toward the field side of the rail seat as the L/V ratio increases; this coincides with a shift in the centroid of loading from the center of the rail seat 1.88 in (47.78 mm) toward the field side, or 1.25 in (31.75 mm) from the field side shoulder at 0.5 L/V.

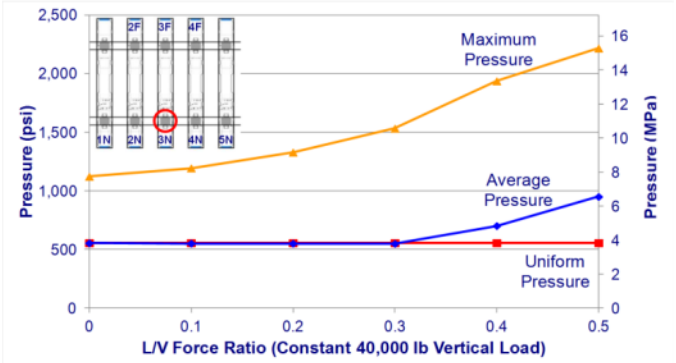

FIGURE 6. CHANGE IN PRESSURE AT 40,000 LB (178 KN) VERTICAL WHEEL LOAD

From the field data, we see that while the assumed range of 400 to 1,800 psi (2.76 MPa and 12.41 MPa) bounds the average pressure exerted on the rail seat under typical loads for North American heavy-axle freight traffic, it does not capture the maximum pressures observed at high lateral loads (above 0.4 L/V). Wear patterns of mild or newly-formed RSD suggest that RSD first develops at these areas of extreme pressure, expanding as the loss of material becomes more severe. More detailed analysis of the characteristics of abrasion at higher pressures, perhaps as high as 2,400 psi (16.55 MPa), and how they differ from the characteristics of lower-pressure abrasion could lead to a better understanding of abrasion as a failure mechanism for RSD.

CONCLUSIONS

Data from field experimentation shows that as lateral load increases, the rail seat becomes more irregularly loaded, and the load distribution concentrates on the field side of the rail seat. At a critical L/V force ratio, the rail seat begins to experience a reduction in contact area. The contact area continues to reduce as lateral load is increased beyond the critical L/V force ratio; at 0.5 L/V it can be seen that the gauge side of the rail seat can be completely unloaded. This further concentrates the rail seat load onto the field side, which could explain the shape of the telltale triangular RSD wear pattern.

Although the modeling work performed by Volpe is relatively basic and relies on several worst-case assumptions, when comparing it to the field results presented in this paper, it provides an acceptable first estimate for the critical L/V force ratio for a loading environment representative of North American heavy-axle load freight. However, at lower vertical loads, the calculated critical L/V tends to overestimate that which is observed in field experimentation. With further refinement, the footing model proposed by Volpe could provide a good basis for a mechanistic calculation of the rail seat load. Consideration should be given for the effect of the vertical wheel load and elastic fastener toe loads in resisting the overturning moment created by the lateral wheel load.

The previous research conducted at UIUC provides insight into the causes, effects, and mitigation of abrasion between the rail pad and rail seat. Although the range of pressures chosen

for their experimentation sufficiently bound the observed average pressure on a rail seat, it did not capture the maximum pressures observed, occurring at 0.4 L/V force ratio and above. Further experimentation at these higher pressures may yield more information on the initial formation of RSD. Consideration should be given to conducting similar tests to those already performed, at higher loads and reduced contact areas to simulate these high L/V scenarios.

The load distribution at the rail seat is critical to four of the five RSD failure mechanisms proposed by researchers at UIUC. Therefore, it is critical to further understand how it is affected by changes in the loading environment and track structure. Further analysis could consider the effects of crosstie support conditions, fastening system type, and RSD-induced wear of the rail seat. These findings may provide guidance in controlling the behavior of the load distribution which, in turn, could mitigate the effects of RSD.

ACKNOWLEDGMENTS

This research was primarily funded by United States Department of Transportation (US DOT) Federal Railroad Administration (FRA). The first two authors were supported by a research grant from Amsted RPS. The published material in this report represents the position of the authors and not necessarily that of US DOT. Generous support and guidance has also been provided from the industry partners of this research: Union Pacific Railroad; BNSF Railway; National Railway Passenger Corporation (Amtrak); Amsted RPS / Amsted Rail, Inc.; GIC Ingeniería y Construcción; Hanson Professional Services, Inc.; and CXT Concrete Ties, Inc., and LB Foster Company. J. Riley Edwards has been supported in part by grants to the UIUC Rail Transportation and Engineering Center (RailTEC) from CN, CSX, Hanson Professional Services, Norfolk Southern, and the George Krambles Transportation Scholarship Fund. For providing direction, advice, and resources, the authors would like to thank Christopher Rapp from Hanson Professional Services, Inc, Mauricio Gutierrez from GIC Ingeniería y Construcción, Professor Jerry Rose and Graduate Research Assistant Jason Stith from the University of Kentucky, and Vince Carrara from Tekscan®, Inc. The authors would also like to thank Marc Killion, Tim Prunkard, and Don Marrow from the University of Illinois at Urbana-Champaign for their assistance in laboratory experimentation, and undergraduate research assistant Zachary Ehlers for his assistance in analyzing the data presented in this paper.

REFERENCES

1. Zeman, J. C. Hydraulic Mechanisms of Concrete-Tie Rail Seat Deterioration. University of Illinois at Urbana-Champaign, Urbana, Illinois, M.S. Thesis 2010.
2. Van Dyk, B. J., M. S. Dersch, and R. E. J. International Concrete Crosstie and Fastening System Survey -- Final Results. Railroad Transportation and Engineering Center (RailTEC), University of Illinois at Urbana-Champaign, Urbana, Illinois, Report submitted to United States Department of Transportation (USDOT) Federal Railroad Administration (FRA) 2012.
3. National Transportation Safety Board. Derailment of Amtrak Train No. 27. National Transportation Safety Board, Washington, D.C., Accident Report RAB-06-03, 2006.
4. Choros, J., M.N. Coltman, and B. Marquis. Prevention of Derailments due to Concrete Tie Rail Seat Deterioration. in *Joint Rail Conference & International Combustion Engine Spring Technical Conference*, Pueblo, Colorado, March 2007, p. 8.
5. Shurpali, A. A. R.G. Kernes, J.R. Edwards, M.S. Dersch, D.A. and C. P. L. Barkan. 2013. Investigation of the Mechanics of Rail Seat Deterioration (RSD) and Methods to Improve Rail Seat Abrasion Resistance in Concrete Sleepers. In: *Proceedings: 10th International Heavy Haul Association Conference*, New Delhi, India, February 2013, pp. 127-133.
6. Rapp, C. R., J. R. Edwards, M. S. Dersch, C. P.L. Barkan, B. Wilson, and J. Mediavilla. Measuring Concrete Crosstie Rail Seat Pressure Distribution with Matrix Based Tactile Surface Sensors. in *2012 ASME Joint Railroad Conference*, Philadelphia, PA, April 2012, pp. 2-3.
7. Schust, W. C., and J. A. Elkins. Wheel Forces During Flange Climb. in *IEEE/ASME Joint Railroad Conference*, Boston, MA, March 1997, pp. 137-147.
8. Van Dyk, B. J., C. T. Rapp, M. J. Greve, A. Scheppe, M. S. Dersch, and J. R. Edwards. Loading Quantification Document. Railroad Transportation and Engineering Center (RailTEC), University of Illinois at Urbana-Champaign, Urbana, Illinois, submitted to United States Department of Transportation (USDOT) Federal Railroad Administration (FRA) 2013.